ARMY RESEARCH LABORATORY

Energy Balance Model for Imagery and Electromagnetic Propagation: Revised

by Henry Rachele
Arnold Tunick

Battlefield Environment Directorate

ARL-TR-522

July 1994

Approved for public release; distribution is unlimited.

NOTICES

Disclaimers

The findings in this report are not to be construed as an official Department of the Army position, unless so designated by other authorized documents.

The citation of trade names and names of manufacturers in this report is not to be construed as official Government indorsement or approval of commercial products or services referenced herein.

Destruction Notice

When this document is no longer needed, destroy it by any method that will prevent disclosure of its contents or reconstruction of the document.

REPORT DOCUMENTATION PAGE

Form Approved
OMB No. 0704-0188

1. AGENCY USE ONLY *(Leave blank)*	2. REPORT DATE July 1994	3. REPORT TYPE AND DATES COVERED Final

4. TITLE AND SUBTITLE
Energy Balance Model for Imagery and Electromagnetic Propagation: Revised

5. FUNDING NUMBERS

6. AUTHOR(S)
Henry Rachele and Arnold Tunick

7. PERFORMING ORGANIZATION NAME(S) AND ADDRESS(ES)
U.S. Army Research Laboratory
Battlefield Environment Directorate
White Sands Missile Range, New Mexico 88002-5501

8. PERFORMING ORGANIZATION REPORT NUMBER
ARL-TR-522

9. SPONSORING / MONITORING AGENCY NAME(S) AND ADDRESS(ES)
U.S. Army Research Laboratory
Battlefield Environment Directorate
White Sands Missile Range, New Mexico 88002-5501

10. SPONSORING / MONITORING AGENCY REPORT NUMBER
ARL-TR-522

11. SUPPLEMENTARY NOTES

12a. DISTRIBUTION / AVAILABILITY STATEMENT
Approved for public release; distribution is unlimited.

12b. DISTRIBUTION CODE

13. ABSTRACT *(Maximum 200 words)*

The optical turbulence structure parameter C_n^2 typically appears in equations used to estimate the effects of temperature and moisture (gradients) on imagery and electromagnetic propagation. Temperature and moisture gradients can be approximated from sensible and latent heat flux estimates, by the application of basic Obukhov similarity theory parameterizations, and the fluxes can be obtained from radiation/energy balance equations. Numerous energy balance models exist requiring different kinds and numbers of inputs. The semiempirical model developed and presented in this report was constrained to require a minimum number of conventional measurements at a reference level (2 m). These measurements include temperature, pressure, relative humidity, and windspeed. The model also requires a judgment of soil type and moisture (dry, moist, or saturated), cloud characteristics (tenths of cloud cover and density and an estimate of cloud height), day of the year, time of day, and longitude and latitude of the site. Model estimates of net radiation, sensible, ground, and latent heat fluxes are compared with measured values. Comparisons of C_n^2 estimates computed from measured versus modeled energy fluxes are also made.

14. SUBJECT TERMS	15. NUMBER OF PAGES
optical turbulence, atmospheric surface layer, sensible heat flux, radiation and energy balance, latent heat flux	55
	16. PRICE CODE

17. SECURITY CLASSIFICATION OF REPORT	18. SECURITY CLASSIFICATION OF THIS PAGE	19. SECURITY CLASSIFICATION OF ABSTRACT	20. LIMITATION OF ABSTRACT
Unclassified	Unclassified	Unclassified	SAR

Acknowledgment

We thank Frank V. Hansen of the Army Research Laboratory for his enthusiastic support and encouragement during the development of the model. He searched out many pertinent documents and gave his time for discussion. We especially appreciate his efforts in compiling albedo and roughness length data for our tables.

Contents

Figures

Figures (continued)

Tables

1. Introduction

This report updates the radiation/energy balance model. [1] Most of the original model concepts and equations are retained; however, a few significant modifications and additions have been made. The changes include an expanded and corrected table of soil thermal constants, tables of surface roughness, albedo values, [2,3], and a dramatically improved method for bridging the fluxes through the sunrise neutral period. Finally, we have corrected editorial errors in the earlier report.

The optical turbulence structure parameter, C_n^2, appears in equations used to estimate the effects of atmospheric turbulence on imagery and electromagnetic (EM) propagation. For many optical systems C_n^2 corresponds with degradation of performance. [4,5,6] Basic equations of C_n^2 [5,7,8,9,10,11] include the real index of refraction gradient as a coefficient, which is a function of the temperature and moisture gradients (preferably potential temperature and specific humidity according to Tatarski [5]). Temperature and moisture gradients can be approximated from sensible and latent heat flux estimates, and the fluxes can be obtained from radiation/energy balance formations.

Numerous radiation/energy balance models appear in the literature [12,13,14,15,16,17,18] varying from comparatively simple to academically complex and requiring different amounts and numbers of inputs and computer capabilities. This report presents a model (hereafter known as the RT model) that was developed for imaging and EM propagation applications when minimum atmospheric information is available. This report also provides the concept and equations that make up the second formalized version of the model. Other reports will follow as the model evolves.

The primary outputs of the RT model are estimates of sensible and latent heat fluxes, which in turn, are used for estimating gradients of potential temperature and specific humidity, making use of Monin-Obukhov similarity relations. These gradients are then used to estimate the optical turbulence parameter C_n^2 needed in the imaging and propagation equations.

The remainder of this report is structured into the following sections: Model Concept, Model Equations, Computational Procedure, Model Results, Discussion, Summary and Conclusions, and References.

2. Model Concept

The following model concept is taken from the operational scenario. An interest is developed in estimating the optical turbulence C_n^2 at a site for different times of a day. The day of interest is known, and the longitude and latitude of the site are known. The soil type may be determined from the USDA Soil Conservation Service's soil maps. Soil wetness (dry, moist, or wet) may be determined from meteorological reports. However, if the soils taxonomy and meteorological reports are not available, on-the-spot judgments are made by examining samples of soil from the surface to 10 cm below the surface. A judgment of sky conditions is also made; in particular, amount of cloud cover (in tenths from 0 to 1), cloud height, and density or sun blocking capacity of the clouds (0 to 3). From the information, estimations are made for net radiative flux, sensible heat, ground heat, and latent heat fluxes using the convention and equations of radiation and energy balance proposed by Carson. [18]

2.1 Radiation Balance Concepts

Carson [18] states that the net radiation flux R_N at the soil surface is equal to the sum of the net short-wave radiative flux, R_{SN}, and the net long-wave radiative flux, R_{LN};

$$R_N = R_{SN} + R_{LN}. \tag{1}$$

The short- and long-wave fluxes are illustrated in figure 1.

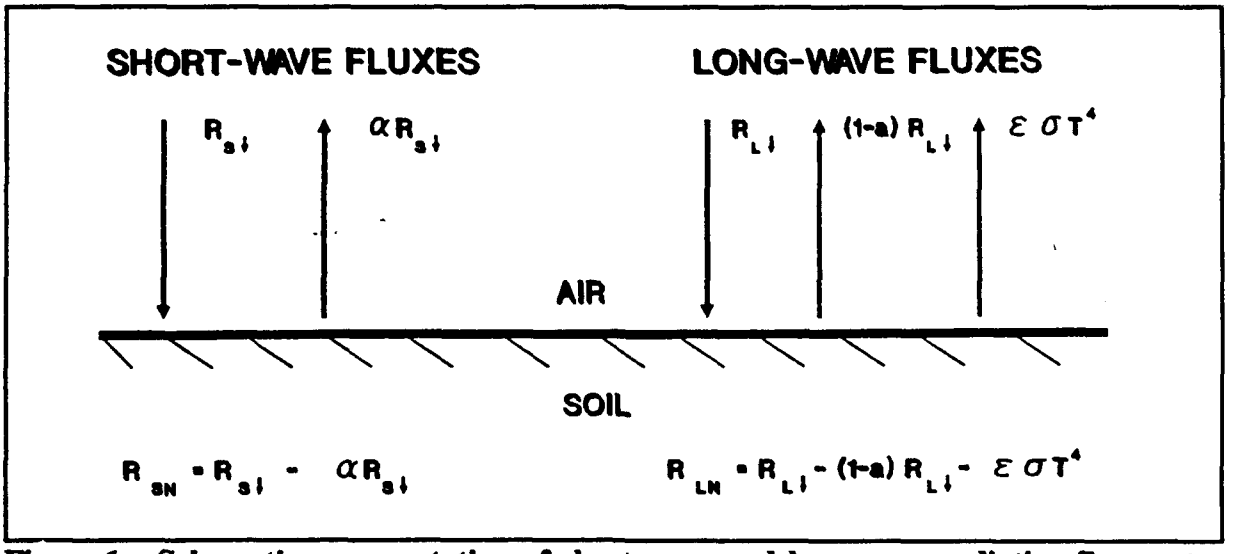

Figure 1. Schematic representation of short-wave and long-wave radiative fluxes at a bare-soil surface.

In figure 1, $R_{s\downarrow}$ is the downward short-wave radiative flux (including both the direct solar flux and diffuse radiation from the sky). However, some of the short-wave radiation is reflected at the surface of the earth so that

$$R_{SN} = R_{S\downarrow} - \alpha R_{S\downarrow}, \tag{2}$$

where

α = the surface short-wave reflectivity (albedo).

Albedo is not as simple as it appears in equation 2; it is a function of soil type, color, vegetative cover and the elevation angle of the sun. Values of α as a function of soil and vegetation are given in tables 1a through 1c, mainly from an extensive compilation by Hansen [2] and Pielke [15]; the functional form of α, relative to the position of the sun, is given in section 3 (Model Equations).

Carson [18] notes that if $R_{L\downarrow}$ is the downward long-wave radiation and a is the surface absorptivity to long-wave radiation, the net incoming flux from the atmosphere is ($a R_{L\downarrow}$). Using Stefan's law, the upward flux caused by thermal emission at the surface of the earth can be written as

$$\epsilon \sigma T_g^4$$

where

T_g = the effective surface temperature
ϵ = the long-wave emissivity at the surface
σ = the Stefan-Boltzman constant.

Hence, the net long-wave radiative flux, R_{LN}, is

$$R_{LN} = a R_{L\downarrow} - \epsilon \sigma T_g^4 \tag{3}$$

where

σ = 5.6697×10^{-8}.

It is common practice to combine the definition of ϵ with Kirchhoff's law so that $a = \epsilon$. However, ϵ varies with soil type, vegetation, and snow or water cover as given in table 2 from Pielke. [15]

Table 1a. Typical values of albedo, α, for various surfaces

Surface	α
Snow and Ice	
Snow, fresh fallen	75-95
Snow, thawing	30-65
Snow, old	40-70
Snow, icy	75
Ice, grey	60
Ice, white	75
Ice, water covered	26
Ice, light snow cover	31
Ice, porous and melting	41
Desert shrublands, snow covered	18-19
Conifer forest, snow covered	59-67
Mixed forest, 50 cm snow covered	20
Grasslands, snow covered	46-50
Crops, snow covered	18-19
Tundra, snow covered	59-67
Soils and Rocks	
Soil, dark, plowed, wet	6
Soil, dark, plowed, dry	8
soil, light, plowed, wet	8
Soil, light, plowed, dry	16
Soil, dark, wet	8
Soil, dark, dry	13
Soil, light, wet	10
Soil, light, dry	18
Dark organic soils	10
Dark grey silt	12
Red soils	17
Brown soils	17
Clay, wet	16
Clay, dry	23
Loam, wet	16
Loam, dry	23

Table 1b. Typical values of albedo, α, for various surfaces (continued)

Surface	α
Soils and Rocks (continued)	
Clay loam, wet	19
Clay loam, dry	13
Sandy soil, wet	20
Sandy soil, dry	25
Sand, white, wet	25
Sand, white, dry	35
Peat soils	5-15
Lime	45
Gypsum	55
Lava	10
Granite	12-18
Rock, wet	20
Rock, dry	35
Stone	30
Urban (People-Influenced)	
Road, blacktop	14
Road, stone	15
Road, dirt, wet	18
Road, dirt, dry	35
Road, clay, wet	20
Road, clay, dry	30
Road, asphalt, wet	10
Road, asphalt, dry	15
Parking lot, black top	8
Concrete, new, white	37
Buildings	9
Developed urban area (average)	15
Roof, thatched, new	20
Roof, thatched, old	15
Roof, tiled, dirty	8

Table 1c. Typical values of albedo, α, for various surfaces (continued)

Surface	α
Crops, Natural Terrain and Vegetation	
Fallow field, wet	5-7
Fallow field, dry	8-12
Spring wheat	10-25
Winter wheat	16-23
Rice paddy	12
Sugar cane	15
Cocoa	16
Ground nuts	17
Winter rye	18-23
Beets	18
Maize	18
Tobacco	19
Potatoes, Yams	19
Alfalfa	23-32
Cotton	20-22
Sorghum	20
Lettuce	22
Forest, coniferous	5-15
Forest, deciduous	10-20
Grass, green	26
Meadows, green	10-20
Coniferous trees, dormant	12
Deciduous trees, dormant	12
Tall grass, dormant	13
Mowed grass, dormant	19
Tundra	15-20
Savanna	15
Steppe	20
Sand dune, wet	20-30
Sand dune, dry	35-45

Table 2. Typical values of emissivity, ϵ, for various surfaces

Ground Cover	ϵ
Fresh snow	0.99
Old snow	0.82
Dry sand	0.95
Wet sand	0.98
Dry peat	0.97
Wet peat	0.98
Soils	0.9-0.98
Asphalt	0.95
Concrete	0.71-0.9
Tar and gravel	0.92
Limestone gravel	0.92
Light sandstone rock	0.98
Desert	0.84-0.91
Grass lawn	0.97
Grass	0.90-0.95
Deciduous forests	0.95
Coniferous forests	0.97
Urban area (range)	0.85-0.95

2.2 Surface Energy Flux Balance Concepts

Carson [18] writes the energy flux balance at the soil surface as

$$R_N = H + L'E + G, \tag{4}$$

where

R_N = the net radiative flux
H = the turbulent sensible-heat flux
L'E = the latent-heat flux caused by surface evaporation
G = the flux of heat into the soil.

The sign (directional) convention of equation 4 is shown in figure 2.

Equations for H, L'E, and G are given in section 3 (Model Equations). Having established the basic radiation/energy balance equations and their directional conventions, the equations chosen to evaluate them are discussed. Although a multitude of relations exist to choose from, the expressions that best satisfy constraints necessary for this application are used.

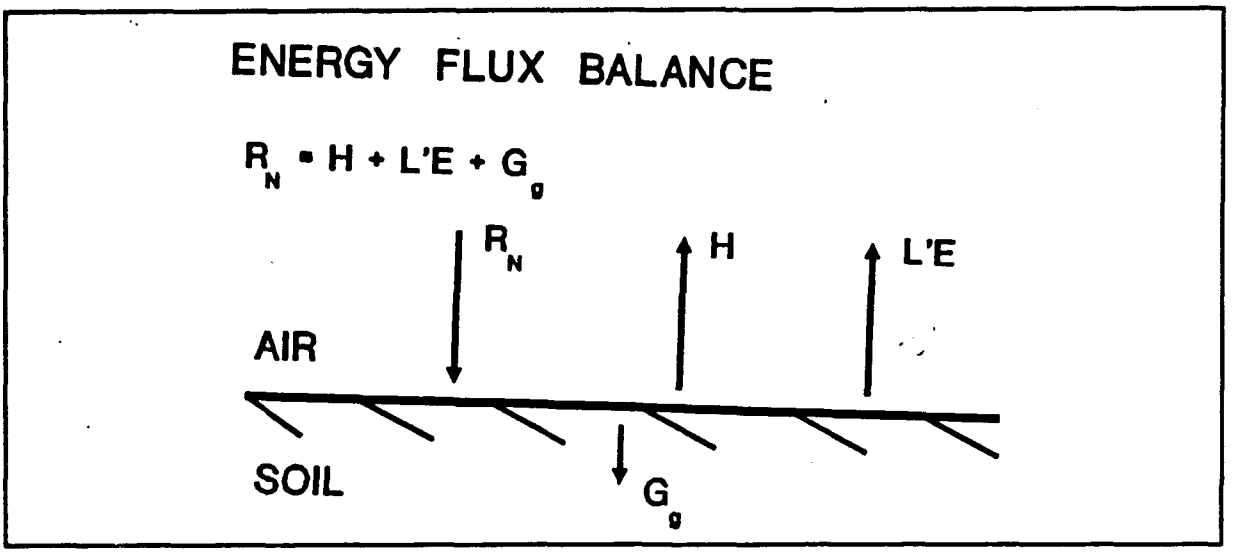

Figure 2. Schematic representation of the energy flux balance at a bare-soil surface.

3. Model Equations

3.1 Short-Wave Solar Radiation

The equations used to compute the incoming short-wave solar radiation for cloudless skies are patterned after Meyers and Dale [19] and Miller and Ricklin. [4] The equations are augmented with empirical results by Haurwitz [20] to account for cloudy skies.

For clear skies Meyers and Dale [19] write

$$R_{S\downarrow} = I = I_o \, T_R \, T_g \, T_w \, T_a \cos Z, \tag{5}$$

where

- I_o = the extraterrestrial flux density at the top of the atmosphere on a surface normal to the incident radiation
- Z = the solar zenith angle
- T_R = the transmission coefficients for Rayleigh scattering
- T_g = absorption by permanent gases
- T_w = water vapor
- T_a = absorption and scattering of aerosols.

The incident radiation, I_o, changes throughout the year because of changes in the earth-sun distance and is adjusted by using the equation

$$I_o = 1353 \, (W \, m^{-2}) \left\{ 1 + 0.034 \cos \left[2\pi \, (n' - 1) / 365 \right] \right\}, \tag{6}$$

where

- n' = the Julian day.

The solar zenith angle is computed by using

$$Z = \cos^{-1} \left\{ \sin (\delta) \sin (D) + \cos (\delta) \cos (D) \cos (H') \right\}, \tag{7}$$

where

- δ = the latitude
- D = the declination angle
- H' = the solar hour angle.

Miller and Ricklin [4] compute the solar declination angle using equations by Woolf [21]:

$$\sin D = \sin (23.4438) \sin \beta, \tag{8}$$

where β in degrees is

$$\beta = \gamma + 0.4087 \sin (\gamma) + 1.8724 \cos (\gamma) - 0.0182 \sin (2\gamma) + 0.0083 \cos (2\gamma) \tag{9}$$

and γ in degrees is

$$\gamma = 279.9348 + d. \tag{10}$$

The angle d is the angular fraction of a year represented by a particular date and may be calculated by

$$d = (\textit{number of day of year} - 1)\ (360/365.242). \tag{11}$$

The solar hour angle H' in degrees is a measure of the longitudinal distance from the sun to the point of calculations given by

$$H' = 15\ (T - M) - \eta, \tag{12}$$

where

T = the Greenwich mean time (GMT) of the calculations
M = the time in hours after midnight of the passage of the sun over the Greenwich meridian or true solar noon
η = longitude, counted positive west of Greenwich.

In terms of d defined in equation 11,

$$M = 12.0 + 0.12357 \sin (d) - 0.004289 \cos (d) + 0.153809 \sin (2d) + 0.060783 \cos (2d) \tag{13}$$

The solar hour angle H' that relates to sunrise and sunset is found using equation 7 as

$$H' = \arccos \left\{ \frac{\sin A - \sin \delta \sin D}{\cos \delta \cos D} \right\} \tag{14}$$

where

A = the sunrise/sunset solar elevation angle.

At ground level Woolf [21] sets A = -0.9 degree. The solar day extends from M - H' (sunrise) to M + H' (sunset).

An empirical equation for $T_R T_g$ in equation 5 by Kondartyev [22] and modified by Atwater and Brown [23] to include forward scattering is

$$T_R T_g = 1.021 - 0.084 \left[m (949 P \times 10^{-5} + 0.051) \right]^{1/2}, \quad (15)$$

where

P = the surface pressure (kPa)
m = the optical air mass at a pressure of 101.3 kPa, given by

$$m = 35 (1224 \cos^2 (Z) + 1)^{-1/2} \quad (16)$$

where

Z = the zenith angle.

An expression for computing the broad-band transmission of water vapor absorption by McDonald [24] is

$$T_w = 1 - 0.077 (um)^{0.3}, \quad (17)$$

where

m = the optical air mass (defined above).

The precipitable water vapor, u, is determined using an expression by Smith [25];

$$u = \frac{P_r W_r}{g (\lambda + 1)}, \quad (18)$$

where

P_r = the pressure at the surface of the earth
W_r = the mixing ratio
g = the acceleration caused by gravity

and λ is given in table 3.

A simple treatment used by Meyers and Dale [19] for estimating T_a was proposed by Houghton [26]

$$T_a = X^m, \quad (19)$$

where

m = the optical mass
X = an empirically derived constant (on the order of 0.935).

Table 3. Seasonal and latitudinal mean values of λ

Season Latitudinal Zone (° N)	Winter	Spring	Summer	Fall	Annual Average
0-10	3.37	2.85	2.80	2.64	2.91
10-20	2.99	3.02	2.70	2.93	2.91
20-30	3.60	3.00	2.98	2.93	3.12
30-40	3.04	3.11	2.92	2.94	3.00
40-50	2.70	2.95	2.77	2.71	2.78
50-60	2.52	3.07	2.67	2.93	2.79
60-70	1.76	2.69	2.61	2.61	2.41
70-80	1.60	1.67	2.24	2.63	2.03
80-90	1.11	1.44	1.94	2.02	1.62
Northern Hemisphere Average	2.52	2.64	2.62	2.70	2.61

To account for the effect of clouds, a transmission coefficient, derived empirically by Haurwitz, [20] is introduced. Haurwitz computed the ratio of insolation with partly or completely covered sky to insolation of cloudless skies, as shown in table 4. Table 4 is used to correct estimates of insolation for cloud cover.

At this point, equations are available for computing the incoming short-wave solar radiation $R_{s\downarrow}$, which is adjusted for albedo. As indicated in table 1, albedo is a function of soil type, color, moisture, vegetation, and solar elevation angle. Although the first four effects are reflected in table 1, the last is computed by using an approximation by Paltridge and Platt [27];

$$\alpha(Z) = \alpha_1 + (1 - \alpha_1) \exp\left[-k' (90^\circ - Z)\right], \tag{20}$$

where

α_1 = the small zenith angle value of albedo
Z = the solar zenith angle

and k' is of order 0.1.

Table 4. Ratio of insolation with partly or completely cloud-covered sky to the insolation with cloudless sky, in percent

	Cloud Amounts Tenths														
	1-3				4-7			8-9			10				
	Density														
Air Mass	0	1	2	3	1	2	3	1	2	3	0	1	2	3	4
1.0	104	103	98	88	98	93	88	92	76	68	87	80	60	31	18
1.5	99	100	97	90	96	89	83	92	75	65	88	79	58	30	19
2.0	94	98	96	92	94	85	78	92	75	63	88	79	55	28	20
2.5	90	96	94	94	92	81	74	92	74	60	89	79	52	27	20
3.0	85	94	92	96	90	78	69	93	74	58	89	79	50	27	21
3.5	81	92	90	98	87	74	65	93	73	56	90	79	47	25	21
4.0	77	90	89	100	84	71	61	93	72	54	90	79	46	25	22
4.5	73	88	87	102	82	67	58	93	72	52	91	79	44	24	23
5.0	70	86	85	104	80	64	54	93	72	50	91	79	41	23	23

3.2 Downward Long-Wave Radiation

Gates [28] offers an expression for downward long-wave radiation for clear skies based on an empirical relationship by Swinbank. [29]

$$R_{L\downarrow} = -170.9 + 1.195\ \sigma\ T_r^4, \tag{21}$$

where

R = watts per meter^2
σ = 5.6697×10^{-8}
T_r = the reference level temperature (K).

Paltridge and Platt [27] suggest an addition to equation 21 to account for clouds, giving a total expression of

$$R_{L\downarrow} = -170.9 + 1.195\ \sigma\ T_r^4 + 0.3\ \epsilon_c\ \sigma\ T_c^4\ (cc), \tag{22}$$

where

ϵ_c = the emissivity of the cloud base (given in table 5)
T_c = the temperature of the cloud base (K).

Having an estimate of the cloud height, T_c can be approximated assuming an average of the dry and moist adiabatic lapse rate. Recent experience has shown that the empirically based constant in equations 21 and 22 can be adjusted to obtain improved radiation estimates before sunrise and after sunset. Modifying the value of the empirically based constant from -170.9 to -130.0 has been somewhat successful.

Table 5. Mean short-wave planetary albedo, α_{ci}, and long-wave flux emissivity, ϵ_{ci}

Cloud Level	Cloud Type	α_{ci}	ϵ_{ci}
1	Cirrus	0.35	0.3
2	Alatocumulus-altostratus	0.55	0.9
3	Low cloud 2	0.60	1.0
4	Low cloud 1	0.50	1.0

3.3 Upward Long-Wave Radiation

The upward long-wave radiative flux $R_{L\uparrow}$ is computed using an equation from Yamada [17] and is expressed as

$$R_{L\uparrow} = \epsilon_g \sigma T_g^4 + (1 - \epsilon_g) R_{L\downarrow}, \tag{23}$$

where

ϵ_g = the surface emissivity (see table 2)
σ = the Stefan-Boltzman constant.

An estimate of the effective ground temperature T_g is required to evaluate equation 23. Obukhov [30] similarity theory parameterizations are applied to reach the estimate. For daytime, unstable surface layer conditions, it is assumed that a semiempirical expression of the sensible heat flux, H, given by Angus-Leppan [31] (based on the Penman [32]) combination form) is adequate as a first approximation for clear skies and dry ground. Angus-Leppan's expression is

$$H = 450\ C\ W \sin \phi_e, \tag{24}$$

where

C = the correction factor (figure 3) for amount of cloud cover
W = the correction factor (figure 3) for amount of ground wetness
ϕ_e = the solar elevation angle ($\phi_e = 90 - Z$).

In equation 24, C = W = 1 for clear skies and dry ground.

For stable conditions, night or day, it is assumed that H is constant and negative in sign. Although this is a relatively weak attempt at modeling the complexities of the sensible heat flux and its associated surface layer temperature gradient structure during stable conditions, it allows the application of a modeling effort to a 24-h data set with some degree of confidence. Literature suggests that in many cases the sensible heat flux remains relatively flat or uniform in the stable surface layer. [31]

Having a first estimate for H, the similarity forms for the Obukhov length, L, and friction velocity, u*, are computed using

$$L = \frac{-u^{*3}\ C_p\ \rho\ \theta_w}{kgH} \tag{25}$$

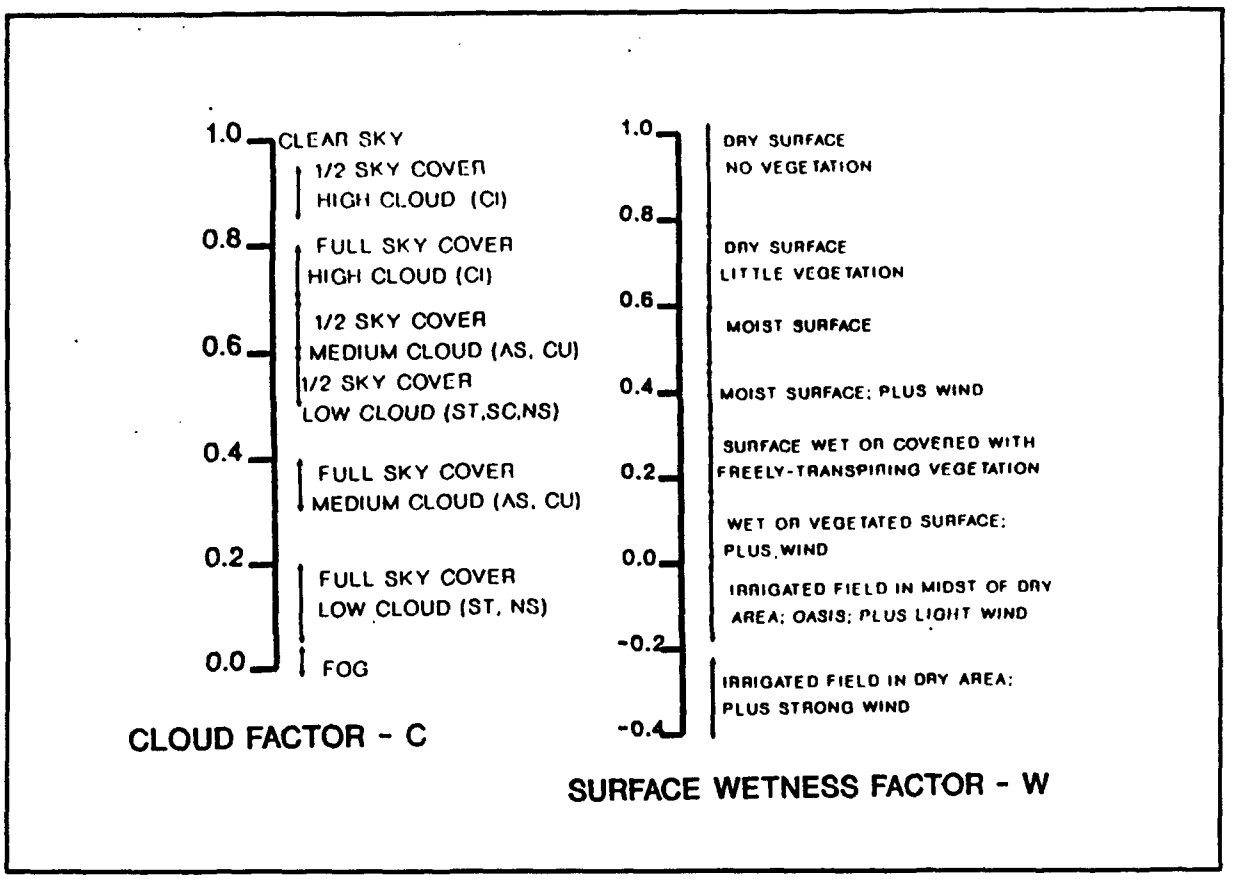

Figure 3. Estimation of parameters C and W.

where

C_p = the specific heat of air

ρ = the density of air

θ_{vr} = the reference level potential temperature

k = Karman's constant (0.4)

g = acceleration caused by gravity, and

$$u^* = V_r\, k \left[\left\{ \ln \left[\frac{x-1}{x+1} \right] + 2 \tan^{-1} x \right\} \Big|_{zo}^{z-d} \right]^{-1}, \qquad (26a)$$

where

V_r = the reference level wind speed

$x = (1 - 5 \frac{z}{L})^{1/4}$ for unstable conditions

$x = 1 + 5 \frac{z}{L}$ for stable conditions.

For neutral conditions

$$u^* = V_r k \left[\ln \frac{z-d}{z_0} \right]^{-1}. \tag{26b}$$

In equations 26a and 26b,

z_0 = the roughness length for momentum
d = the displacement height.

Approximate values for these parameters can be estimated by $z_0 = 0.14\ z_e$ and $d = 0.7\ z_e$, where z_e is referred to as the height of the roughness element or the average height of the terrain or ground cover (surface vegetation). Table 6 represents an extensive compilation by Hansen [3] of typical roughness length values for various surfaces.

Iteratively solving equations 25 and 26a or 26b obtains values for L and u* for the approximated value of H. From similarity forms, it can be written

$$\theta^* = \frac{u^{*2}\,\theta_{vr}}{kgL}. \tag{27}$$

Hence, a first estimate for θ^*, the potential temperature scaling constant, can be computed and used to approximate T_g because

$$T_g = T(z) - \frac{\theta^*}{k} \left\{ \ln \left[\frac{y-1}{y+1} \right] \right\} \Big|_{z_h}^{z-d} \tag{28a}$$

where

$y = (1 - 15\ \frac{z}{L})^{1/2}$ for unstable conditions

$y = 1 + 5\ \frac{z}{L}$ for stable conditions.

For neutral conditions

$$T_g = T(z) - \frac{\theta^*}{k} \left\{ \ln \frac{z-d}{z_h} \right\}. \tag{28b}$$

Table 6a. Typical values of roughness length, Z_0, for various surfaces

Type of Surface	Z_0 (cm)
Ice	0.001
Smooth mud flats	0.001
Dry lake bed	0.003
Tundra, snow covered	0.01
Tundra, patchy snow	0.03
Tundra, after snow melt	0.40
Tundra, mid-summer	2.40
Snow cover (Antarctic)	0.01
Calm open sea	0.01
Desert, smooth	0.03
Grass, closely mowed	0.10
Grass, short	0.14
Farmland, snow covered	0.20
Bare soil, tilled	0.20-0.60
Nebraska prairie	0.70
Sparse grass, 10 cm high	0.70
Thick grass, 5-6 cm high	0.75
Grassy plains, level topography	1.0
Kansas prairie	1.0
Low shrubs, level topography	2.6
Grasslands, 18 cm high	2.7
Uncut grass w/isolated trees	3.0
Grass and trees, mixed	3.5
Sparse brush, semi-arid	5.0
Sparse grass, 50 cm high	5.0
Thick grass, 50 cm high	9.0
Thick grass, 60-70 cm high	8.10-15.0
Brush, scrub growth, open	16.0
Brush, scrub growth, dense	25.0
Wooded country, level topography	40.0
Forested plateau, level topography	70.0-120.0
Forested plateau, rolling hills	120.0-130.0
Low mountains, hills, unforested	75.0
Subtropical Savannah, grass, few trees	31.0-41.0
Subtropical Savannah, grass w/many shrubs	51.0-61.0
Coniferous forest	110.0

Table 6b. Typical values of roughness length, Z_0, for various surfaces (continued)

Type of Surface	Z_0 (cm)
Alfalfa	2.7
Cashew orchard, 2 m high	3.5-4.0
Potatoes, 60 cm high	4.0
Farmland, few trees	6.0
Farmland, many hedges	8.0
Bean crop, 1.2 m high	7.4
Cotton, 1.27 m high	13.0
Wheat	22.0
Citrus orchard	31.0-40.0
Corn, 2.2 m high	74.0
Blacktop, concrete	0.002
Airport runways	3.0
Highways, railways	50.0
Villages, towns	40.0-50.0
Residential, low density	110.0
City park	130.0
Urban buildings, business district	175.0-320.0
High rise apartments	370.0

However, to evaluate equation 28a or 28b an estimate of Z_h (the roughness length for temperature) is required, which is determined from the modification of Verma [33] and is expressed as

$$Z_h = \frac{L}{15}\left\{1 - \left[\frac{1 + B^*}{1 - B^*}\right]^2\right\}, \tag{29}$$

where

$$B^* = \left[\frac{y(z-d)+1}{y(z-d)-1}\right] e^{(kB^{-1}+A)}, \tag{30}$$

$$A = \left\{\ln\left[\frac{x-1}{x+1}\right] + 2\tan^{-1}x\right\}\Big|_{zo}^{z-d}; \tag{31}$$

$$y = \left[1 - 15 \frac{Z}{L} \right]^{1/2}, \; x = \left[1 - 15 \frac{Z}{L} \right]^{1/4} \tag{32a}$$

for unstable conditions,

$$y = x = 1 + 5 \frac{Z}{L} \tag{32b}$$

for stable conditions, and

$$Z_h = 0.13 Z_o \tag{33}$$

for neutral conditions.

In practice, it is common to approximate $Z_h = 0.13 Z_o$ at all times of the day including transition or neutral periods. Values for kB^{-1} (where k is Karman's constant and B is the Stanton number [34]) for different soil surfaces and vegetation are given in figure 4.

Having an estimate of T_g for dry cloudless conditions, $R_{L\uparrow}$ is computed. From the above equations, the first estimate of net radiation can be computed.

3.4 Ground Heat Flux

In Rachele and Tunick, [1] the ground heat flux is expressed as

$$G = - G^* + \left(T_g - T_{gn} \right) K_o \sin \left\{ \frac{\pi}{12} \left(t - t_n \right) \right\}, \tag{34}$$

where

$$G^* = [T_g(t_n + 2) - T_{gn}] K_o \sin\{\pi/12[(t_n + 2) - t_n]\} \tag{35}$$

T_{gn} = ground temperature during adiabatic conditions (approximately 1 h after sunrise)

tn = time (relative to midnight) of adiabatic conditions

$K_o = \frac{Ks}{2\sqrt{K}}$ for soil type and wetness

Ks = soil thermal conductivity (W m^{-1} K^{-1})

K = soil thermal diffussivity (m^2 h^{-1}).

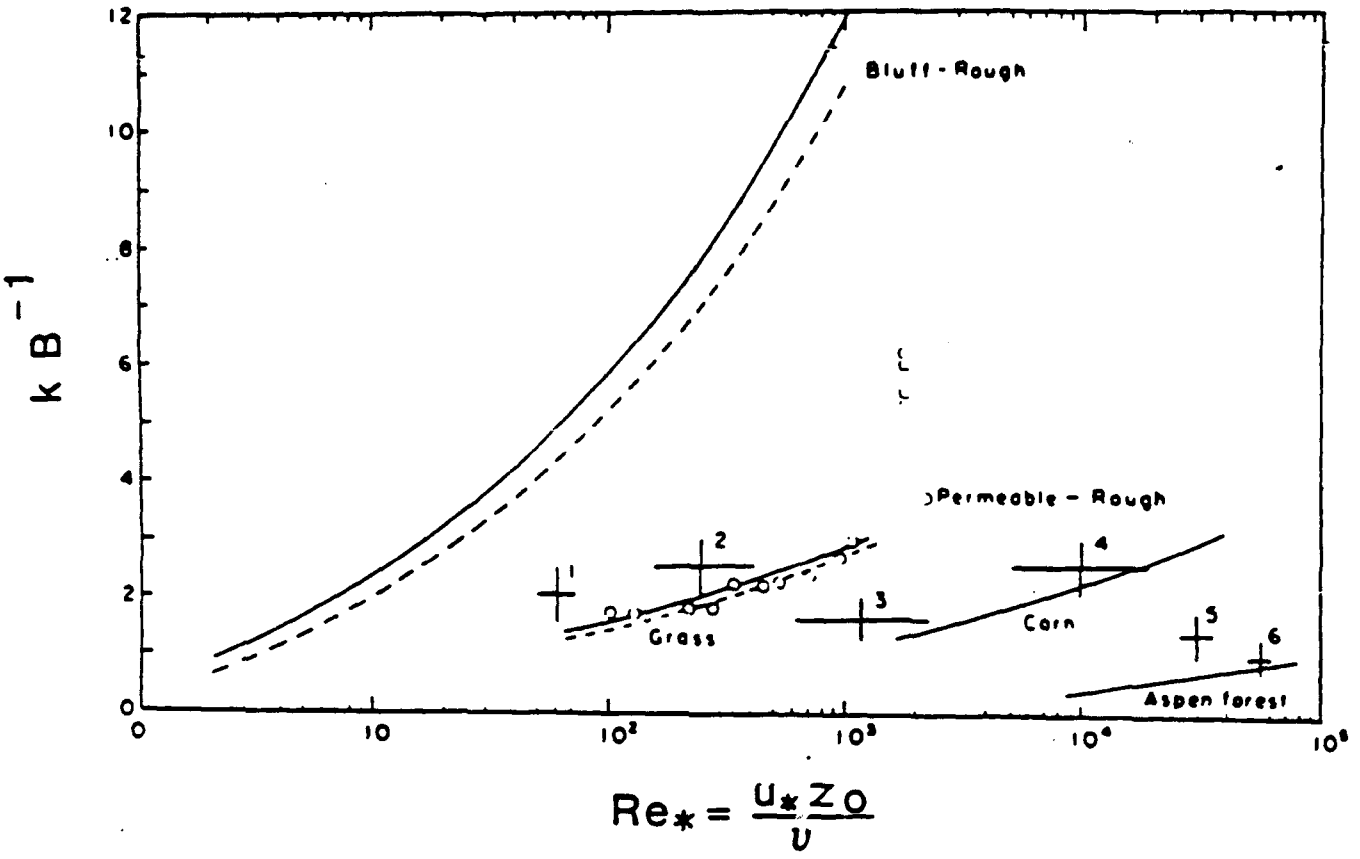

Figure 4. kB^{-1} is a function of the roughness Reynolds number, $Re^* = u^*Z_o/\upsilon$ (adapted from W. Brutsaert, 1984, *Evaporation in the Atmosphere*, D. Reidel Publishing Company, Dordrecht).

Equations 34 and 35 are modifications to the expressions for ground heat flux given by Angus-Leppan and Brunner. [12] Table 7 contains values of thermal constants newly compiled by Rachele for this report.

Equation 35 implies that the ground heat flux is zero approximately 2 h after the neutral period, and approximately 3 h after sunrise. More recent experience confirms that the morning transition period may be approximated by $T_{sunrise}$ + 1 h and that G^* can often be set to a constant value (for example, $G^* \approx 11.0 - 15.0$).

The equations necessary for computing a second approximation for H, assuming that for clear skies and dry ground conditions the latent heat flux is negligible, are now available. Let $H = R_n - G$ and complete an iterative process to determine a dry H. In the second half of the computations, cloud cover on net radiative fluxes, soil moisture on ground heat storage, and evaporation and wind

Table 7. Average thermal properties of soils, rock, snow, ice, and water[a]

Material	State	K_s (W m^{-1} K^{-1})	K (m^2 hrs^{-1})	K_o
Sand	Dry	0.277	9.000×10^{-4}	5.0
Sand	Moist	2.0	2.520×10^{-3}	20.8
Sand	Saturated	2.2	2.120×10^{-3}	24.3
Quartz Sand (Medium Fine)	Dry	0.264	7.200×10^{-4}	5.037
Quartz Sand	8.3% Moist	0.586	1.188×10^{-3}	8.7
Yolo Silt Loam	Dry	0.12	4.500×10^{-4}	2.79[b]
Yolo Silt Loam	Moist	0.44	1.860×10^{-3}	5.23[b]
Yolo Silt Loam	Saturated	0.848	1.730×10^{-3}	10.44[b]
Sandy Loam	Dry	0.23	5.760×10^{-4}	4.9
Sandy Soil	Saturated	2.2	2.660×10^{-3}	21.8
Sandy Clay	15% Moist	0.925	1.330×10^{-3}	12.98
Clay Soil	Dry	0.3	5.490×10^{-4}	6.28
Clay Soil	Moist	1.47	3.960×10^{-3}	11.71
Clay Soil	Saturated	1.58	1.840×10^{-3}	18.90
Clay Pasture	—	2.76	4.320×10^{-3}	21.50
Calcareous Soil (Calcium Carbonate)	43% Water	0.712	6.480×10^{-4}	13.94
Soil (Generic)	Very Dry	0.167-0.345	$7.2\text{-}11.0 \times 10^{-4}$	3.19-5.37
Soil (Generic)	Wet	1.260-3.350	$1.44\text{-}3.6 \times 10^{-4}$	17.0-28.6
Mud	—	0.84	7.920×10^{-4}	15.28
Peat Soil	Dry	0.13	5.400×10^{-4}	2.65
Peat Soil	Saturated	0.85	$4.320.10^{-4}$	20.95
Concrete	—	0.92	1.730×10^{-3}	11.33
Granite	0° C	2.72	4.570×10^{-3}	20.60
Limestone	0° C	2.00	2.920×10^{-3}	18.96
Marble	—	2.30	3.490×10^{-3}	19.92
Sandstone	—	2.60	4.070×10^{-3}	20.87
Snow	Fresh	0.08	3.600×10^{-4}	2.16
Snow	Old	0.42	1.440×10^{-3}	5.67
Ice	—	2.24	4.180×10^{-3}	17.75
Water	4° C	0.57	5.040×10^{-4}	13.00

[a]These values represent coarse averages of values taken from Oke, [35] Campbell, [14] Geiger, [36] Danard, [16] Van Wijk, [37] Lettau and Davidson, [38] and the Smithsonian Meteorological Tables. [39]

[b]These values are adjusted to approximate surface values.

speed on sensible heat estimates are considered. Section 4 provides a step-by-step procedure for computing the dry and wet sensible and ground heat fluxes and the net radiation using equations presented above. The latent heat flux, L'E, is estimated by the model as a residual. Latent heat flux is expressed as $L'E = R_n - H - G$.

4. Computational Procedure

This section presents a flowchart (figure 5) and step-by-step method description of the computational procedure. For the procedure, the following are assumed to be known at a geographical site selected for computing estimates of sensible and latent heat fluxes: (1) longitude and latitude of the site; (2) day of year and time of day; (3) reference level (2 m) values of temperature (T_r), pressure (P_r), relative humidity (f_r), and horizontal windspeed (V_r); (4) measure or judgment of cloud cover (cc) in tenths and cloud density on a scale of 0 to 3 (3 being most dense); (5) albedo of the soil, including vegetative cover; (6) composition and wetness of the soil (dry, moist, saturated); and (7) estimate of cloud type and height.

Step 1: Compute the elevation angle $\phi = 90° - Z$ of the sun at the times of interest using Woolf's [21] equations (equations 7 through 13).

Step 2: Compute a first approximation of the sensible heat flux H_d for dry ground and cloudless skies using Angus-Leppan and Brunner [12]

$$H_d = 45 C W \sin \phi_e \tag{36}$$

(for C = W = 1 in figure 3)

Step 3: Compute the friction velocity, u^*, and the Obukhov length, L (equations 25 and 26a or 26b).

Step 4: Compute the potential temperature scaling constant θ^* using equation 27 repeated here as

$$\theta^* = u^{*2} \theta_{vr} / kgL, \tag{37}$$

where

$$\theta_{vr} = T_r(1 + 0.61 q_r) \tag{38}$$

and

$$q_r = 3.8x10^{-3} \frac{f_r}{100} exp\left(5.44x10^3\left(\frac{1}{273.15} - \frac{1}{T_r}\right)\right). \tag{39}$$

Step 5: Knowing T_r, θ_*, and L, compute the effective ground temperature T_g at height Z_h using equations 28 through 32c.

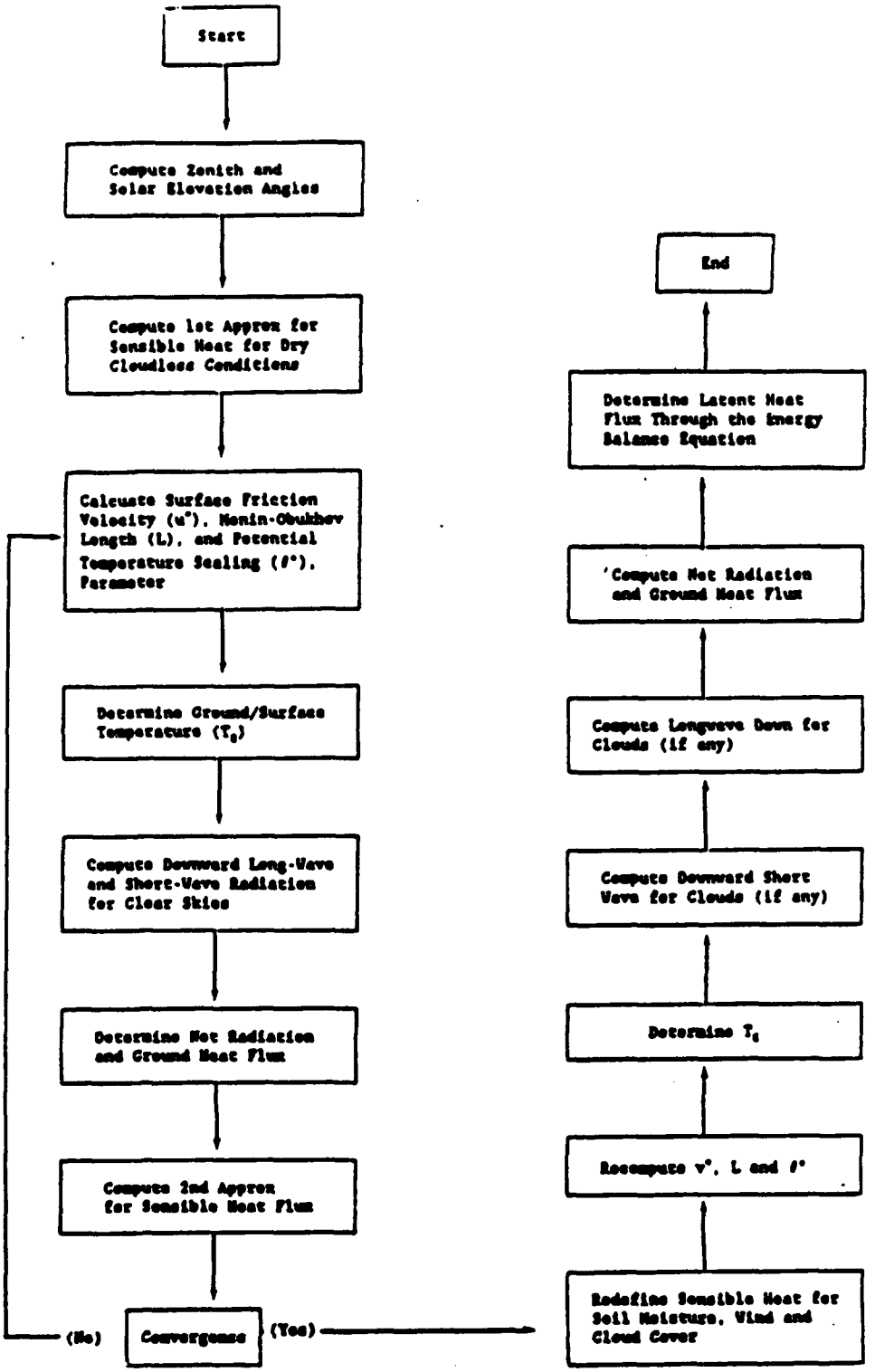

Figure 5. Flowchart of computational procedure.

Step 6: Compute the downward long-wave radiation for clear skies (equation 31) using Swinbank. [29]

Step 7: From Meyers and Dale [19], compute $R_{s\downarrow}$ for cloudless skies as in equations 5 through 19.

Step 8: Compute sunrise and sunset time using Woolf's [21] equations (equations 13 and 14).

Step 9: Compute the incoming insolation after surface reflection, $(1 - \alpha)\ R_{s\downarrow}$, from Paltridge and Platt. [27] Equation 20 is repeated here as

$$\alpha = \alpha_1 + (1 - \alpha_1) \exp [-k'(90° - Z)], \tag{40}$$

where

k'	=	0.1
Z	=	zenith angle
α_1	=	albedo at high solar elevations.

Step 10: Compute the upward long-wave radiation $R_{L\uparrow}$ using Yamada, [17] as in equation 23.

Step 11: Compute a first approximation for the net radiation (steps 1 through 10) as

$$R_N = (1 - \alpha)\ R_{S\downarrow} - (R_{L\uparrow} - R_{L\downarrow}). \tag{41}$$

Step 12: Compute $T_g - T_{gn}$ using $T_{gn} = T_m + \gamma_d\ (Z_r - (Z_h + d))$
where

T_{gn}	=	the temperature in degrees kelvin at Z_h
γ_d	=	the dry adiabatic lapse rate
T_m	=	the reference height temperature at the time t_n (relative to midnight) of neutral conditions.

This temperature difference will be used to compute a first estimate of the dry ground heat flux, G_d.

Step 13: Compute dry value of G (G_d) using an equation by Rachele and Tunick (see equations 34 and 35 and table 7).

Step 14: For strictly unstable surface layer conditions, compute a second approximation of H_d using

$$H_d = R_N - G_d. \tag{42}$$

Recall that the sensible heat flux, H, remains constant for stable conditions while $H = 0$ during transition periods.

Step 15: Repeat Steps 2 through 14 until convergence is attained, giving dry values of H, R_N, and G.

Step 16: For unstable conditions, redefine H as $H = H_d\ C\ W$.

Step 17: Determine C and W from Angus-Leppan and Brunner [12] (figure 3) as a function of cloud cover, soil wetness, and wind speed.

Step 18: Alternatively, for grassy, damp vegetative ground cover, compute H using the Rachele/Tunick empirically derived function

$$H = H_d\ C\ W(V_r), \tag{43}$$

where $W(V_r)$ is shown on figure 6 (RT modified Angus-Leppan, Brunner plot).

Step 19: Compute u^*, θ^*, L, T_g using corrected values of H.

Step 20: If necessary, compute $R_{s\downarrow}$ for cloudy skies using table 4 from Haurwitz. [20]

Step 21: If necessary, recompute $(1 - \alpha)\ R_{s\downarrow}$.

Step 22: If necessary, recompute $R_{L\downarrow}$ for cloud cover (equation 22).

Step 23: Compute $R_{L\uparrow}$ using the newly computed value of T_g.

Step 24: Recompute

$$R_N = (1 - \alpha)\ R_{S\downarrow} - (R_{L\uparrow} - R_{L\downarrow}). \tag{44}$$

Step 25: Recompute $T_g - T_{gn}$.

Step 26: Recompute a value for G using expressions in equations 34 and 35 with the appropriate values for the thermal constants outlined in table 7.

Step 27: Compute the latent heat flux L'E as $L'E = R_n - G - H$.

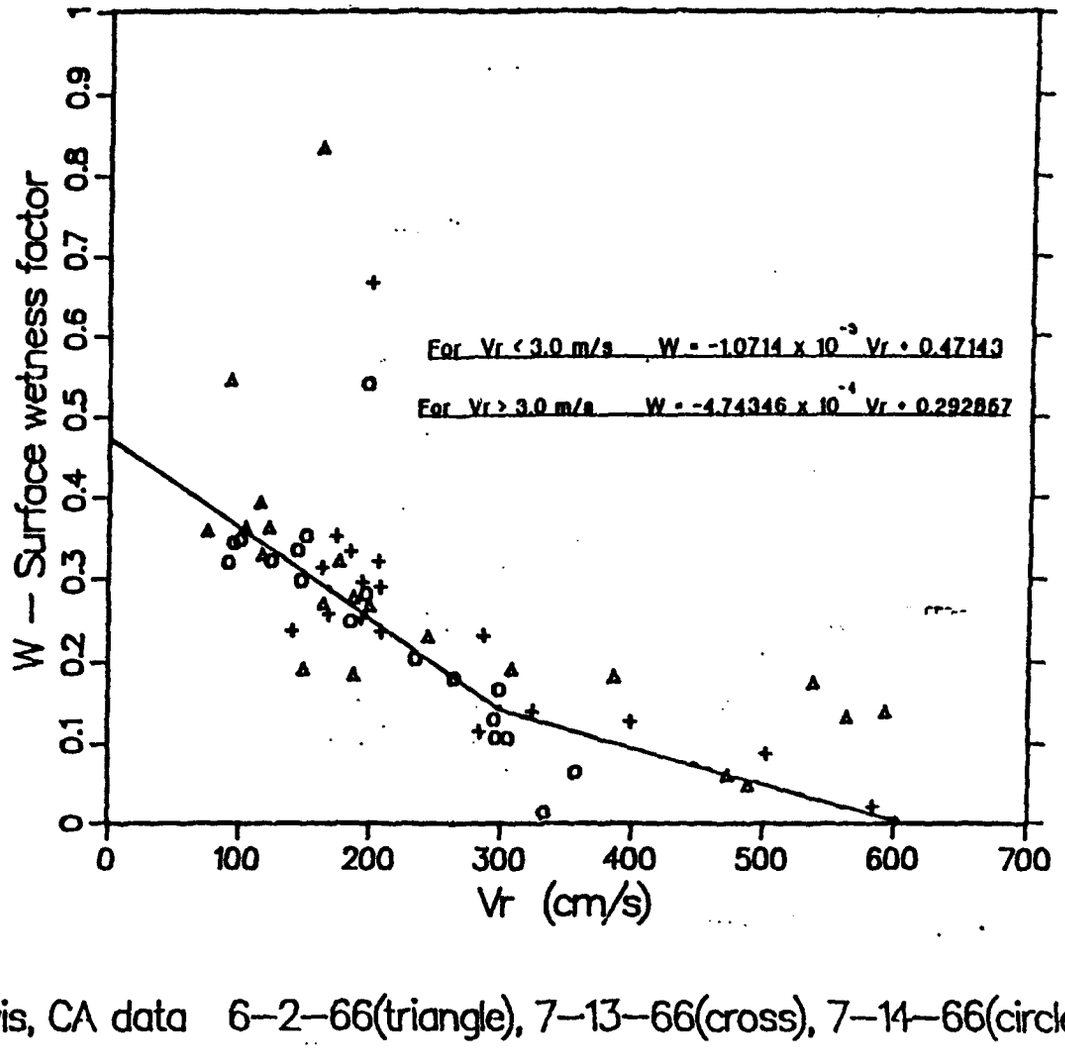

Figure 6. The Rachele/Tunick function $W(V_r)$ (a modified Angus-Leppan and Brunner Plot).

5. Model Results

The results of this study are based on three sets of measured data (1/2-h averages) collected at Davis, CA, during summer 1966 and spring 1967. [40,41,42] The Davis field site, a flat, 5-ha area, at 17 m above sea level, is located about 2 km west of the main part of the University of California at the Davis Campus, 24 km west of Sacramento, and 113 km northeast of San Francisco. Data were taken when the surrounding fields were mostly crop covered and well irrigated, giving homogenous surface conditions with respect to temperature and moisture. Advection effects were considered negligible. Profiles of wind, temperature, and moisture were measured with transducers at nine levels from 25 to 600 cm. Raw data were processed to give 1/2-h average profiles.

In addition, 1/2-h values of net radiation and sensible, latent, and soil heat fluxes were available. The terrain at Davis was relatively smooth and covered with fescue grass (average height 10 cm). The soil was assumed to be a moist, silt loam. Two data sets were collected during cloudless sky conditions.

Figure 7 shows 1/2-h average values of reference level temperature, relative humidity, and windspeed for the 3 days. Figures 8, 9, and 10 show the measured and model values of sensible, latent, and ground heat fluxes for each day. Figure 11 shows the measured and modeled net radiation for each day. Figure 12 shows the results for the numerically approximated optical turbulence structure parameter (in the visible) for each day, using measured versus modeled fluxes for inputs.

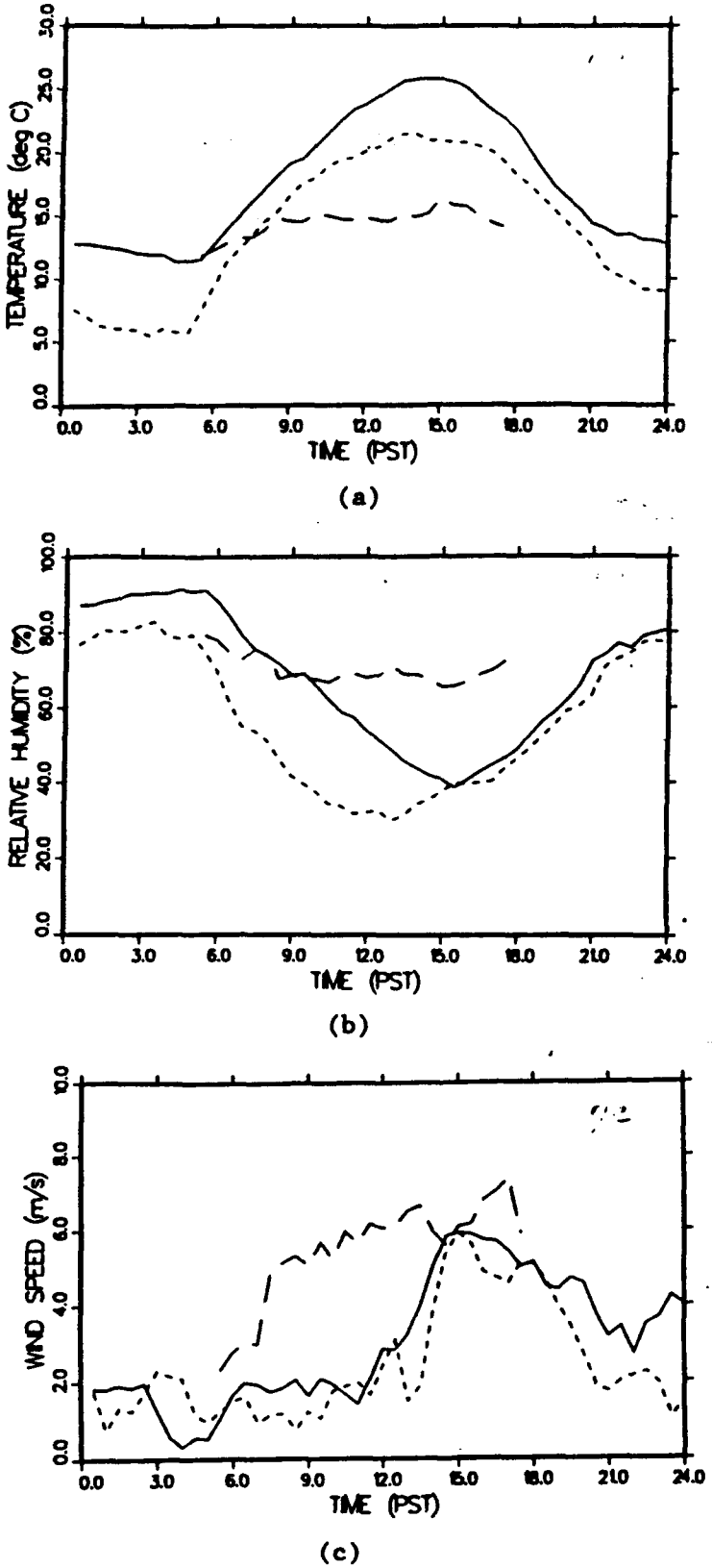

Figure 7. 1/2-hr average values of reference level (2 m) (a) temperature, (b) relative humidity, and (c) windspeed (Davis, CA data) 6-2-66 (small dashed line), 7-13-66 (solid line), 5-9-67 (large dashed line).

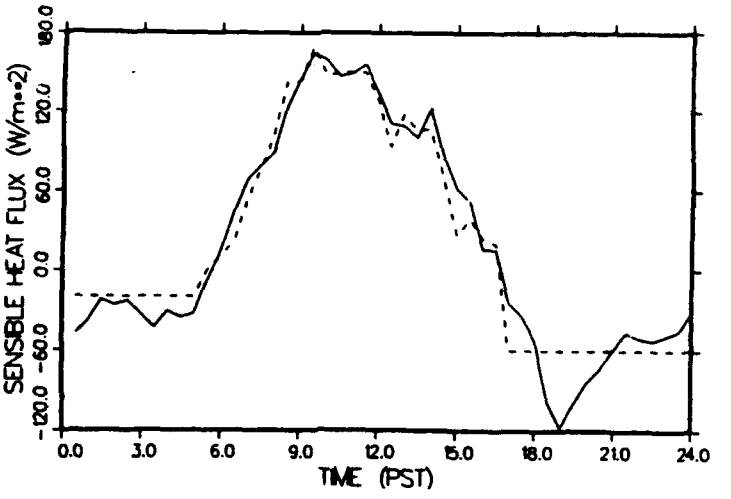

(a)

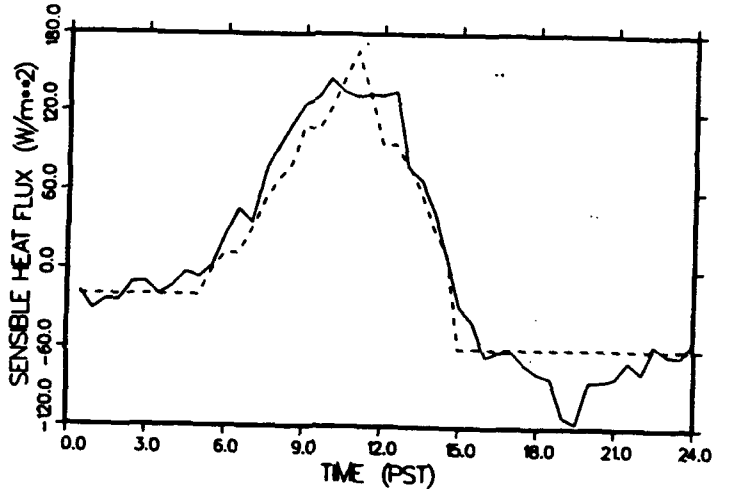

(b)

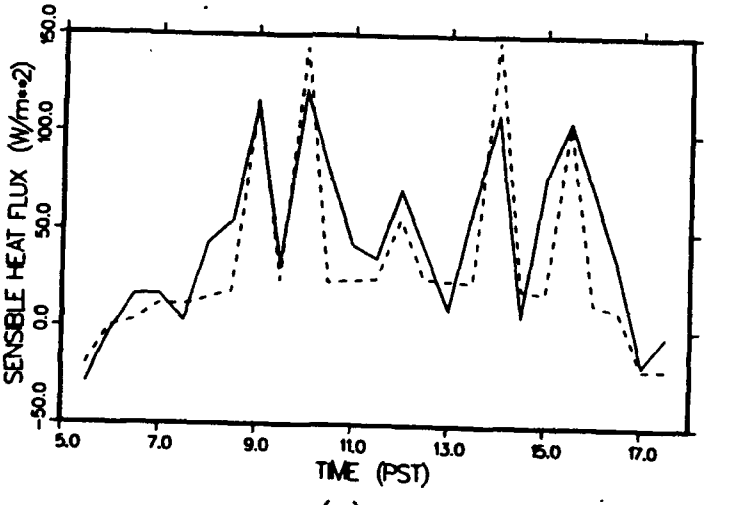

(c)

Figure 8. Measured (solid line) and modeled (dashed line) values of sensible heat for Davis, CA data on (a) 6-2-66, (b) 7-13-66, and (c) 5-9-67.

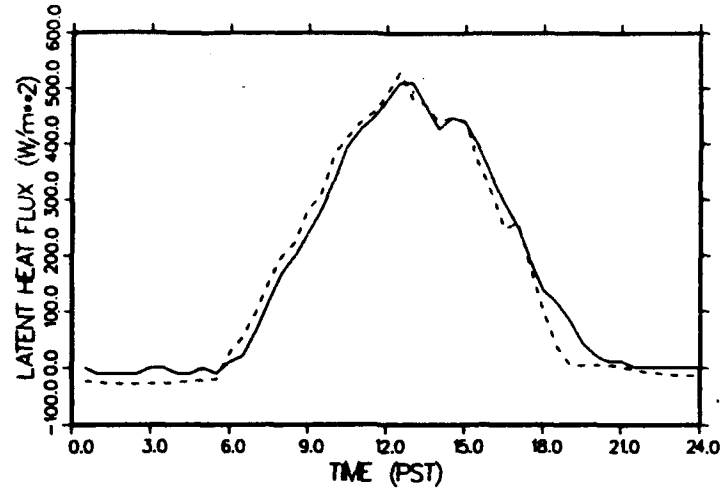

(a)

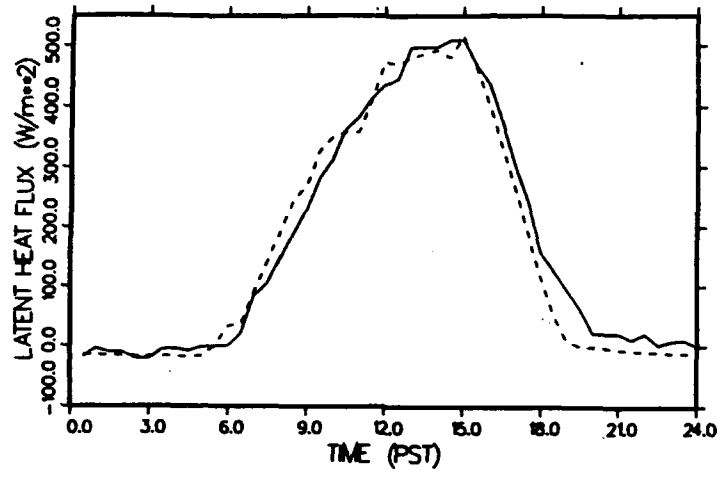

(b)

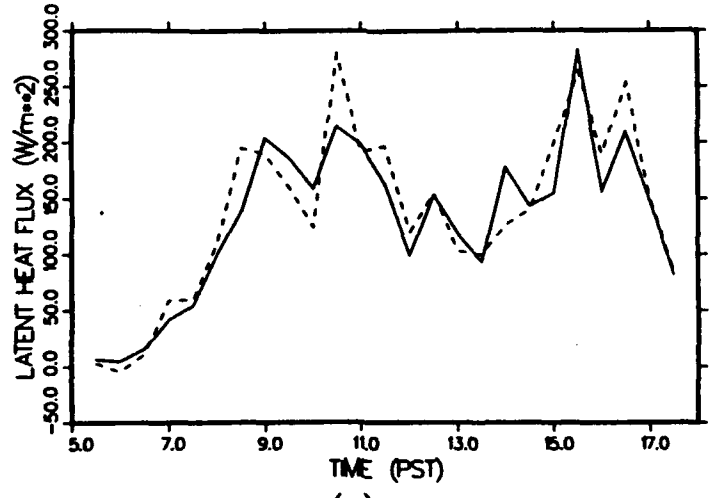

(c)

Figure 9. Measured (solid line) and modeled (dashed line) values of latent heat for Davis, CA data on (a) 6-2-66, (b) 7-13-66, and (c) 5-9-67.

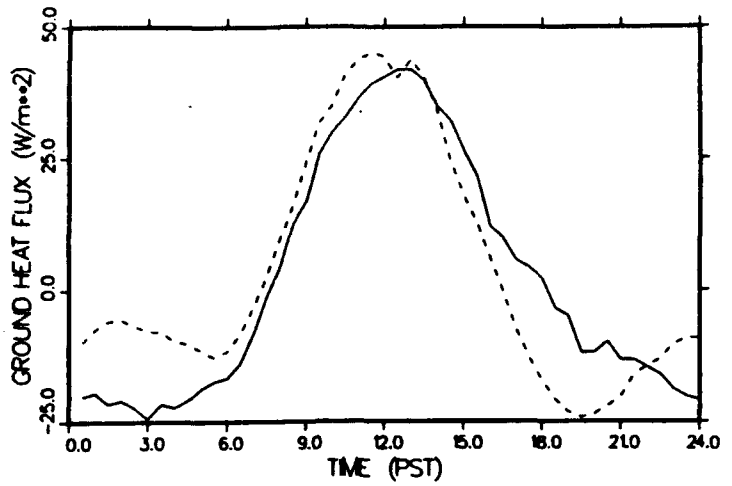

(a)

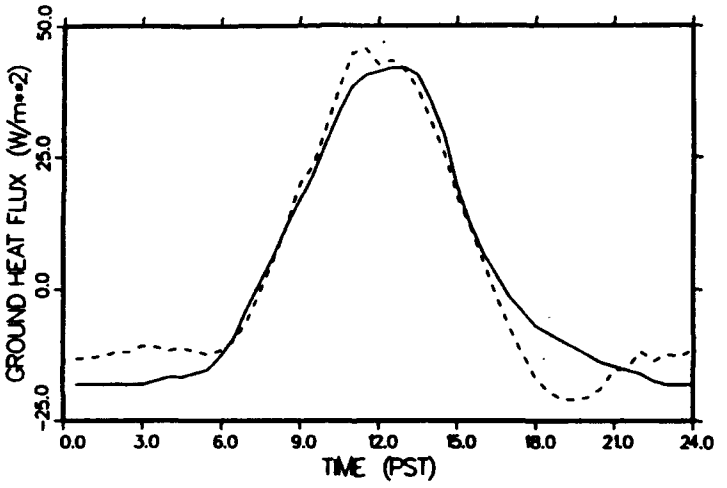

(b)

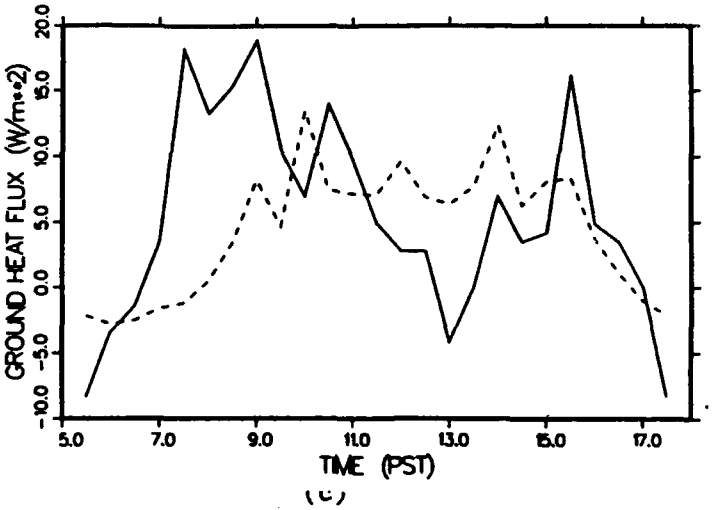

(c)

Figure 10. Measured (solid line) and modeled (dashed line) values of ground heat flux for Davis, CA data on (a) 6-2-66, (b) 7-13-66, and (c) 5-9-67.

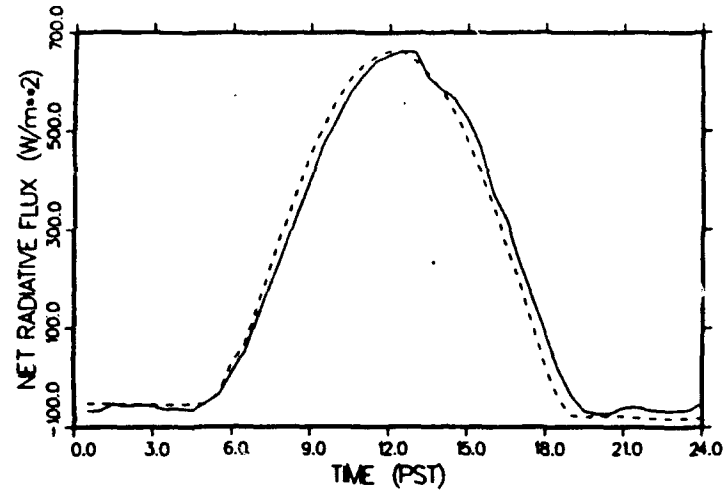

(a)

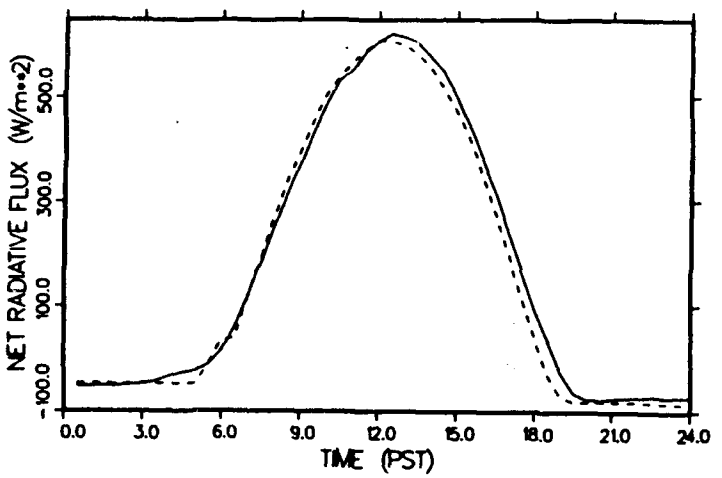

(b)

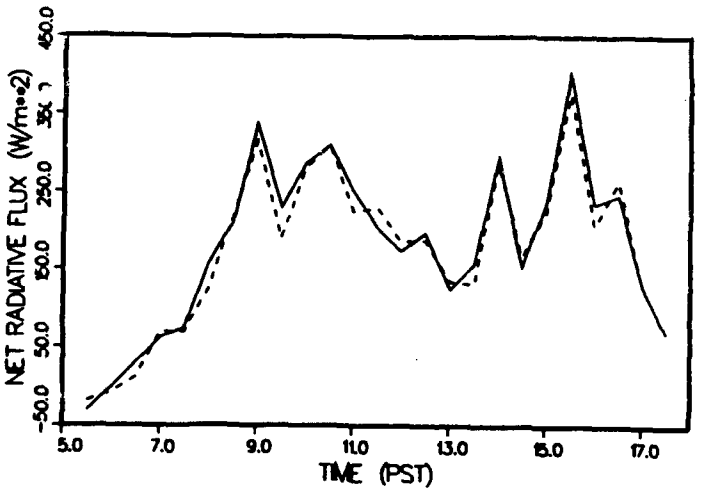

(c)

Figure 11. Measured (solid line) and modeled (dashed line) values of net radiative flux for Davis, CA data on (a) 6-2-66, (b) 7-13-66, and (c) 5-9-67.

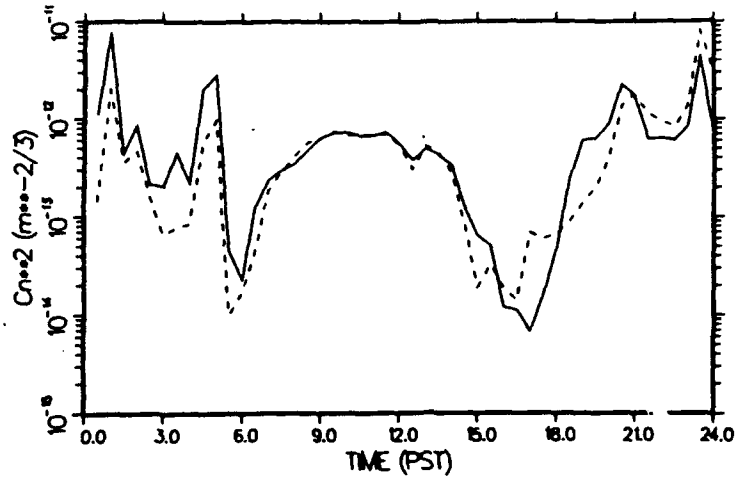

(a)

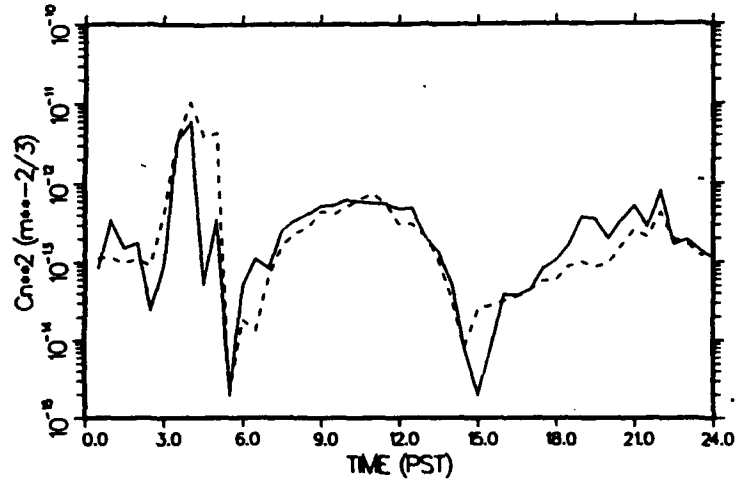

(b)

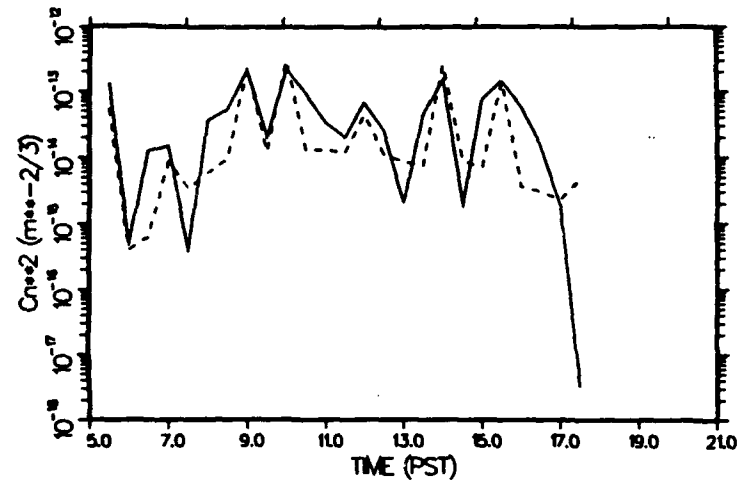

(c)

Figure 12. Optical turbulence structure parameter, C_n^2, for visible wave-lengths for Davis, CA data (a) 6-2-66, (b) 7-13-66, and (c) 5-9-67. Measured fluxes (solid) and modeled fluxes (dashed) as input.

6. Discussion

The model assumes that the sensible heat flux remains constant before sunrise and after sunset; therefore, departures in model estimates from the observed data at these times, as shown in figures 8a and 8b, are not surprising. A relatively uniform heat flux with time from midnight to sunrise, as suggested by Angus-Leppan [31], is observed. With regard to figure 8c, it is clear that the structure of the observed data for the variably cloud covered sky period has been reasonably well represented. Success relies primarily upon the ability to interpret the cloud factor effects as shown in figure 3. The interrelation between the insolation ratios found in table 4 and the cloud factors given in figure 3 must be considered. Application of these corrections for cloud cover depends heavily upon good cloud density information (and the more standard cloud base and cloud type input data). Imagine a partly cloudy sky over a site. The rays of the sun may be mostly blocked. However, it is possible to observe a clear, unobstructed line of sight to the sun, even if 8/10 or 9/10 cloud cover were reported. This basic scenario can make radiation and energy balance modeling extremely difficult, unless more effort is directed toward integrating cloud cover and ground wetness factors (figure 3) with the insolation ratio values of Haurwitz [20] given in table 4.

Agreement between measured versus modeled values of latent heat flux are illustrated in figures 9a, 9b, and 9c. The agreement is good because L'E is computed as the residual of the other estimated energy balance components. A strong dependency on figure 11c (net radiation) is implied by figure 9c.

The best results of ground heat flux estimates are shown in figure 10b. From each figure (10a, 10b, and 10c) it is clear that the expressions applied to the most difficult problem need refinement, especially before sunrise and after sunset. The daytime peak magnitudes are well represented, primarily because of the proper application of the soil thermal constants given in table 7.

The most recognizable successes are illustrated in figures 11a, 11b, and 11c. The equations chosen for making estimates of the net radiative flux were well suited to model constraints and ultimate application to electromagnetic propagation and imagery. A sensitivity to modeling the net radiation under cloud covered skies that relies heavily upon having good cloud density approximations was found. By using the information given in table 4, the calculated shortwave component was adjusted to give better net radiation estimates. It is more difficult to model radiation exchanges when the cloud field is not uniform.

7. Summary and Conclusions

The purpose of this study was to determine the feasibility of structuring a radiation/energy balance model that yields estimates of sensible and latent heat fluxes, suitable for imagery and EM propagation assessments, research, and applications, when constrained to require atmospheric measurement of temperature, pressure, relative humidity, and wind at a reference height (about 2 m).

The model presented satisfies the above constraints; however, one must also know the day of the year, time of day, longitude and latitude of the site of interest, judgment of soil type and moisture (dry, moist, saturated), and cloud characteristics (tenths of cloud cover, density, cloud type, and approximate height).

The model is a composite of equations, some purely physical and well founded, others semiempirical, and a few that are strictly empirical. Major contributions include equations for estimating the effect of wind on the sensible heat flux; an expression for estimating ground heat flux; a modification of Verma's expression for the computation of the roughness length of temperature; and, most critically, tying together the equations and establishing a calculation procedure.

The three cases presented in this report were restricted to using data from Davis, CA to be consistent with our previous report. [1] Results are most encouraging for determining qualitative estimates of the radiation and energy balance fluxes and C_n^2 throughout the day over fescue grass.

It is only fair to say that the model should be used and refined for barren surfaces and other vegetative cover. A joint data collection effort with the U.S. Department of Agriculture, Agricultural Research Service was carried out in May and July, 1992, in Bushland, Texas [43] to serve that purpose.

References

1. Rachele, H. and A. Tunick, 1992, *Energy Balance Model for Imagery and Electro-magnetic Propagation*, ASL-TR-0311, Atmospheric Sciences Laboratory, White Sands Missile Range, NM, 88002-5501.

2. Hansen, F. V., 1993a, *Albedos*, ARL Technical Report (ARL-TR-57), U.S. Army Research Laboratory, Battlefield Environment Directorate, White Sands Missile Range, NM 88002-5501.

3. Hansen, F. V., 1993b, *Surface Roughness Lengths*, ARL Technical Report (ARL-TR-61), U.S. Army Research Laboratory, Battlefield Environment Directorate, White Sands Missile Range, NM 88002-5501.

4. Miller, W. B., and J. C. Ricklin, 1990, "A Module for Imaging Through Optical Turbulence, IMTURB," ASL-TR-0221-27, U.S. Army Atmospheric Sciences Laboratory, White Sands Missile Range, NM.

5. Tatarski, V. I., 1961, *Wave Propagation in a Turbulent Medium*, McGraw-Hill Book Company, Incorporated, New York - Toronto - London.

6. Fried, D. L., 1967, "Propagation of a Spherical Wave in a Turbulent Medium," *J Opt Soc Am*, 57:175-180.

7. Panofsky, H. A., 1968, "The Structure Constant for the Index Refraction in Relation to the Gradient of Index of Refraction in the Surface Layer," *J. Geophys. Res.*, 73(18):6047-6049.

8. Hill, R. J., 1989, "Implications of Monin-Obukhov Similarity Theory for Scalar Quantities," *J Atmos Sci*, 46:2236-2244.

9. Andreas, Edgar L., 1988, "Estimating C_n^2 Over Snow and Sea Ice from Meteorological Data," *J Opt Soc Am*, 5:481-495.

10. Wyngaard, J. C., 1973, "On Surface Layer Turbulence," In *Workshop on Micro-meteorology*, D. A. Haugen (ed) American Meteorological Society, Boston, MA, pp 101-149.

11. Wesely, M. L., 1976, "The Combined Effect of Temperature and Humidity Fluctuations on Refractive Index," *J. Appl. Meteorol.*, 15:43-49.

12. Angus-Leppan, P. V., and F. K. Brunner, 1980, "Atmospheric Temperature Models for Short-Range EDM," *The Canadian Surveyor*, 34(2):153-165.

13. Webb, E. K., 1984, "Temperature and Humidity Structure in the Lower Atmosphere," *Geodetic Refraction - Effects of Electromagnetic Wave Propagation Through the Atmosphere*, F. K. Brunner, ed, Springer Publishing, Berlin, Heidelberg, New York, Tokyo, pp 85-141.

14. Campbell, G. S., 1985, *Soil Physics with Basic: Transport Models for Soil-Plant Systems*, Elsevier Publishing Company, Amsterdam, Oxford, New York, Tokyo.

15. Pielke, R. A., 1984, *Mesoscale Meteorological Modeling*, Academic Press, Orlando, San Diego, San Francisco, New York, London, Tokyo, Toronto, Montreal, Sydney.

16. Danard, M., G. Lyv, and G. MacGillivray, 1984, "A Mesoscale Bulk Model of the Atmospheric Boundary Layer," Atmospheric Dynamics Corporation Report, Victoria, British Columbia, Canada.

17. Yamada, T., 1981, "A Numerical Study of Turbulent Air Flow in and Above Forest Canopy," *J. Met. Soc. Jap.*, 60(1):439-454.

18. Carson, D. J., 1987, "An Introduction to the Parameterization of Land-Surface Processes: Part 1. Radiation and Turbulence," *Meteorological Magazine No. 1381*, 116:229-242.

19. Meyers, T. P., and R. F. Dale, 1983, "Predicting Daily Insolation With Hourly Cloud Height and Coverage," *J. Clim and Appl. Meteorol.*, 22:537-545.

20. Haurwitz, B., 1945, "Insolation in relation to cloudiness and cloud density," *J. Meteorol*, 2(3):154-166.

21. Woolf, H. M., 1968, "On the Computation of Solar Elevation Angles on the Determination of Sunrise and Sunset Times," National Meteorological Center, Environmental Sciences Services Administration, Hillcrest Heights, MD.

22. Kondratyv, K. Ya, 1969, *Radiation in the Atmosphere*, Academic Press, New York, and London, p 912.

23. Atwater, M. A., and P. Brown, 1974, "Numerical Calculation of the Latitudinal Variation of Solar Radiation for an Atmosphere of Varying Opacity," *J Appl Meteorol*, 13:289-297.

24. McDonald, J. E., 1960, "Direct Absorption of Solar Radiation by Atmospheric Water Vapor," *J. Meteorol.*, 17:319-328.

25. Smith, W. L., 1966, "Note on the Relationship Between Total Precipitable Water and Surface Dew Point," *J. Appl. Meteorol.*, 5:726-727.

26. Houghton, H. G., 1954, "On the Annual Heat Balance of the Northern Hemisphere," *J. Meteorol.*, 11:1-9.

27. Paltridge, G. W., and C. M. R. Platt, 1976, *Radiative Processes in Meteorology and Climatology*, Elsevier Scientific Publishing Company, Amsterdam, Oxford, New York.

28. Gates, D. M., 1965, "Radiant Energy, Its Receipt and Disposal," in *Meteorological Monographs, Agricultural Meteorology*, American Meteorological Society, Boston, MA, 6(28):1-26.

29. Swinbank, W.C., 1963, "Longwave Radiation From Clear Skies," *Quart. J. Roy Met. Soc.*, 89:339-348.

30. Obukhov, A.M., 1971, Turbulence in an Atmosphere with a Non-uniform Temperature, *Boundary-Layer Meteor.*, Vol. 2, 7-29 (Russian original, 1946).

31. Angus-Leppan, P. V., 1971, "Meteorological Physics Applied to the Calculation of Refraction Corrections," in *Proceedings of the Conference of Commonwealth Survey Officers*, Cambridge, England, pp 107-111.

32. Penman, H. L., 1948, "Natural Evaporation From Open Water Bare Soil and Grass," in *Proceedings of the Royal Society*, London, 193:120-145.

33. Verma, S. B., 1989, "Aerodynamic Resistances to Transfers of Heat, Mass, and Momentum," *Estimation of Areal Evapotranspiration* (Proceedings of a Workshop held in Vancouver, BC, Canada, August 1987) IAHS Publication No. 177.

34. Brutsaert, W., 1984, *Evaporation into the Atmosphere*, D. Reidel Publishing Company, Dordrecht.

35. Oke, T. R., 1978, *Boundary Layer Climates*, Methuen, NY.

36. Geiger, R., 1959, *The Climate Near the Ground*, Harvard University Press, Cambridge, MA.

37. Wilk, W. R. van, 1963, "General Temperature Variations in a Homogeneous Soil," *Physics of Plant Environment*, North-Holland.

38. Lettau, H. H., and B. Davidson, 1957, *Exploring the Atmosphere's First Mile*, Vol. 2, Pergamon Press, Oxford.

39. Smithsonian Meteorological Tables, 1951, *R. J. List.*

40. Stenmark, E. B., and L. D. Drury, 1970, *Micrometeorological Field Data From Davis, California 1966-67, Runs Under Non-Advective Conditions*, ECOM-6051, U.S. Army Electronics Command, Atmospheric Sciences Laboratory, Fort Huachuca, AZ.

41. Brooks, F. A., et al., 1968, *Analysis in Transfers of Energy, Momentum and Moisture Near the Ground*, ECOM-66-G26-F, U.S. Army Electronics Command, Atmospheric Sciences Laboratory, Fort Huachuca, AZ.

42. Morgan, D. L., et al., 1970, *Evaporation From an Irrigated Turf Under Advection of Dry Air at Davis, California*, ECOM-68-G10-1, U.S. Army Electronics Command, Atmospheric Sciences Laboratory, Fort Huachuca, AZ.

43. Tunick, A., H. Rachele, F.V. Hansen, T.A. Howell, J.L. Steiner, A. Scheider, and S.R. Evett, 1994, "REBAL'92 - A Cooperative Radiation and Energy Balance Feild Study for Imagery and E.M. Propagation," (accepted to be published in March, 1994 issue) *Bulletin of the American Meteorological Society.*

Bibliography

Campbell, G. S., 1977, *An Introduction to Environmental Biophysics*, Springer Verlag, New York.

Liu, M. et al., 1976, "The Chemistry Dispersion and Transport of Air Pollutants Emitted From Fossil Fuel Plants in California: Data Analysis and Emission Impact Model," PB-264-822, National Technical Information Center, Springfield, VA, pp 136-140.

DISTRIBUTION

	Copies
Commandant U.S. Army Chemical School ATTN: ATZN-CM-CC (Mr. Barnes) Fort McClellan, AL 36205-5020	1
NASA Marshal Space Flight Center Deputy Director Space Science Laboratory Atmospheric Sciences Division ATTN: E501 (Dr. Fichtl) Huntsville, AL 35802	1
NASA/Marshall Space Flight Center Atmospheric Sciences Division ATTN: Code ED-41 Huntsville, AL 35812	1
Deputy Commander U.S. Army Strategic Defense Command ATTN: CSSD-SL-L (Dr. Lilly) P.O. Box 1500 Huntsville, AL 35807-3801	1
Deputy Commander U.S. Army Missile Command ATTN: AMSMI-RD-AC-AD (Dr. Peterson) Redstone Arsenal, AL 35898-5242	1
Commander U.S. Army Missile Command ATTN: AMSMI-RD-DE-SE (Mr. Lill, Jr.) Redstone Arsenal, AL 35898-5245	1
Commander U.S. Army Missile Command ATTN: AMSMI-RD-AS-SS (Mr. Anderson) Redstone Arsenal, AL 35898-5253	1
Commander U.S. Army Missile Command ATTN: AMSMI-RD-AS-SS (Mr. B. Williams) Redstone Arsenal, AL 35898-5253	1
Commander U.S. Army Missile Command Redstone Scientific Information Center ATTN: AMSMI-RD-CS-R/Documents Redstone Arsenal, AL 35898-5241	1

Commander
U.S. Army Aviation Center
ATTN: ATZQ-D-MA (Mr. Heath) 1
Fort Rucker, AL 36362

Commander
U.S. Army Intelligence Center
and Fort Huachuca
ATTN: ATSI-CDC-C (Mr. Colanto) 1
Fort Huachuca, AZ 85613-7000

Northrup Corporation
Electronics Systems Division
ATTN: Dr. Tooley 1
2301 West 120th Street, Box 5032
Hawthorne, CA 90251-5032

Commander
Pacific Missile Test Center
Geophysics Division
ATTN: Code 3250 (Mr. Battalino) 1
Point Mugu, CA 93042-5000

Commander
Code 3331
Naval Weapons Center
ATTN: Dr. Shlanta 1
China Lake, CA 93555

Lockheed Missiles & Space Co., Inc.
Kenneth R. Hardy
ORG/91-01 B/255 1
3251 Hanover Street
Palo Alto, CA 94304-1191

Commander
Naval Ocean Systems Center
ATTN: Code 54 (Dr. Richter) 1
San Diego, CA 92152-5000

Meteorologist in Charge
Kwajalein Missile Range
P.O. Box 67 1
APO San Francisco, CA 96555

U.S. Department of Commerce Center
Mountain Administration
Support Center, Library, R-51
Technical Reports
325 S. Broadway 1
Boulder, CO 80303

Dr. Hans J. Liebe
NTIA/ITS S 3
325 S. Broadway 1
Boulder, CO 80303

NCAR Library Serials
National Center for Atmos Research
P.O. Box 3000 1
Boulder, CO 80307-3000

Headquarters
Department of the Army
ATTN: DAMI-POI 1
Washington, DC 20310-1067

Mil Asst for Env Sci Ofc of
the Undersecretary of Defense
for Rsch & Engr/R&AT/E&LS
Pentagon - Room 3D129 1
Washington, DC 20301-3080

Headquarters
Department of the Army
DEAN-RMD/Dr. Gomez 1
Washington, DC 20314

Director
Division of Atmospheric Science
National Science Foundation
ATTN: Dr. Bierly 1
1800 G. Street, N.W.
Washington, DC 20550

Commander
Space & Naval Warfare System Command
ATTN: PMW-145-1G 1
Washington, DC 20362-5100

Director
Naval Research Laboratory
ATTN: Code 4110
(Mr. Ruhnke) 1
Washington, DC 20375-5000

Commandant
U.S. Army Infantry
ATTN: ATSH-CD-CS-OR (Dr. E. Dutoit) 1
Fort Benning, GA 30905-5090

USAFETAC/DNE 1
Scott AFB, IL 62225

Air Weather Service
Technical Library - FL4414 1
Scott AFB, IL 62225-5458

USAFETAC/DNE
ATTN: Mr. Glauber 1
Scott AFB, IL 62225-5008

Headquarters
AWS/DOO 1
Scott AFB, IL 62225-5008

Commander
U.S. Army Combined Arms Combat
ATTN: ATZL-CAW 1
Fort Leavenworth, KS 66027-5300

Commander
U.S. Army Space Institute
ATTN: ATZI-SI 1
Fort Leavenworth, KS 66027-5300

Commander
U.S. Army Space Institute
ATTN: ATZL-SI-D 1
Fort Leavenworth, KS 66027-7300

Commander
Phillips Lab
ATTN: PL/LYP (Mr. Chisholm) 1
Hanscom AFB, MA 01731-5000

Director
Atmospheric Sciences Division
Geophysics Directorate
Phillips Lab
ATTN: Dr. McClatchey 1
Hanscom AFB, MA 01731-5000

Raytheon Company
Dr. Sonnenschein
Equipment Division
528 Boston Post Road 1
Sudbury, MA 01776
Mail Stop 1K9

Director
U.S. Army Materiel Systems Analysis Activity
ATTN: AMXSY-CR (Mr. Marchetti) 1
Aberdeen Proving Ground, MD 21005-5071

Director
U.S. Army Materiel Systems Analysis Activity
ATTN: AMXSY-MP (Mr. Cohen) 1
Aberdeen Proving Ground, MD 21005-5071

Director
U.S. Army Materiel Systems Analysis Activity
ATTN: AMXSY-AT (Mr. Campbell) 1
Aberdeen Proving Ground, MD 21005-5071

Director
U.S. Army Materiel Systems
Analysis Activity
ATTN: AMXSY-CS (Mr. Bradley) 1
Aberdeen Proving Ground, MD 21005-5071

Director
ARL Chemical Biology
Nuclear Effects Division
ATTN: AMSRL-SL-CO 1
Aberdeen Proving Ground, MD 21010-5423

Army Research Laboratory
ATTN: AMSRL-D 1
2800 Powder Mill Road
Adelphi, MD 20783-1145

Army Research Laboratory
ATTN: AMSRL-OP-SD-TP 1
Technical Publishing
2800 Powder Mill Road
Adelphi, MD 20783-1145

Army Research Laboratory
ATTN: AMSRL-OP-CI-SD-TL 1
2800 Powder Mill Road
Adelphi, MD 20783-1145

Army Research laboratory
ATTN: AMSRL-SS-SH 1
(Dr. Sztankay)
2800 Powder Mill Road
Adelphi, MD 20783-1145

U.S. Army Space Technology
and Research Office
ATTN: Ms. Brathwaite 1
5321 Riggs Road
Gaithersburg, MD 20882

National Security Agency
ATTN: W21 (Dr. Longbothum) 1
9800 Savage Road
Fort George G. Meade, MD 20755-6000

OIC-NAVSWC
Technical Library (Code E-232) 1
Silver Springs, MD 20903-5000

Commander
U.S. Army Research office
ATTN: DRXRO-GS (Dr. Flood) 1
P.O. Box 12211
Research Triangle Park, NC 27009

Dr. Jerry Davis
North Carolina State University
Department of Marine, Earth, and
Atmospheric Sciences 1
P.O. Box 8208
Raleigh, NC 27650-8208

Commander
U.S. Army CECRL
ATTN: CECRL-RG (Dr. Boyne) 1
Hanover, NH 03755-1290

Commanding Officer
U.S. Army ARDEC
ATTN: SMCAR-IMI-I, Bldg 59 1
Dover, NJ 07806-5000

Commander
U.S. Army Satellite Comm Agency
ATTN: DRCPM-SC-3 1
Fort Monmouth, NJ 07703-5303

Commander
U.S. Army Communications-Electronics
Center for EW/RSTA
ATTN: AMSEL-EW-MD 1
Fort Monmouth, NJ 07703-5303

Commander
U.S. Army Communications-Electronics
Center for EW/RSTA
ATTN: AMSEL-EW-D 1
Fort Monmouth, NJ 07703-5303

Commander
U.S. Army Communications-Electronics
Center for EW/RSTA
ATTN: AMSEL-RD-EW-SP 1
Fort Monmouth, NJ 07703-5206

Commander
Department of the Air Force
OL/A 2d Weather Squadron (MAC) 1
Holloman AFB, NM 88330-5000

PL/WE 1
Kirtland AFB, NM 87118-6008

Director
U.S. Army TRADOC Analysis Center
ATTN: ATRC-WSS-R 1
White Sands Missile Range, NM 88002-5502

Director
U.S. Army White Sands Missile Range
Technical Library Branch
ATTN: STEWS-IM-IT 3
White Sands Missile Range, NM 88002

Army Research Laboratory
ATTN: AMSRL-BE (Mr. Veazy) 1
Battlefield Environment Directorate
White Sands Missile Range, NM 88002-5501

Army Research Laboratory
ATTN: AMSRL-BE-A (Mr. Rubio) 1
Battlefield Environment Directorate
White Sands Missile Range, NM 88002-5501

Army Research Laboratory
ATTN: AMSRL-BE-M (Dr. Niles) 1
Battlefield Environment Directorate
White Sands Missile Range, NM 88002-5501

Army Research Laboratory
ATTN: AMSRL-BE-W (Dr. Seagraves) 1
Battlefield Environment Directorate
White Sands Missile Range, NM 88002-5501

USAF Rome Laboratory Technical
Library, FL2810 1
Corridor W, STE 262, RL/SUL
26 Electronics Parkway, Bldg 106
Griffiss AFB, NY 13441-4514

AFMC/DOW 1
Wright-Patterson AFB, OH 03340-5000

Commandant
U.S. Army Field Artillery School
ATTN: ATSF-TSM-TA (Mr. Taylor) 1
Fort Sill, OK 73503-5600

Commander
U.S. Army Field Artillery School
ATTN: ATSF-F-FD (Mr. Gullion) 1
Fort Sill, OK 73503-5600

Commander
Naval Air Development Center
ATTN: Al Salik (Code 5012) 1
Warminister, PA 18974

Commander
U.S. Army Dugway Proving Ground
ATTN: STEDP-MT-M (Mr. Bowers) 1
Dugway, UT 84022-5000

Commander
U.S. Army Dugway Proving Ground
ATTN: STEDP-MT-DA-L 1
Dugway, UT 84022-5000

Defense Technical Information Center
ATTN: DTIC-OCP 2
Cameron Station
Alexandria, VA 22314-6145

Commander
U.S. Army OEC
ATTN: CSTE-EFS 1
Park Center IV
4501 Ford Ave
Alexandria, VA 22302-1458

Commanding Officer
U.S. Army Foreign Science & Technology Center
ATTN: CM 1
220 7th Street, NE
Charlottesville, VA 22901-5396

Naval Surface Weapons Center
Code G63 1
Dahlgren, VA 22448-5000

Commander and Director
U.S. Army Corps of Engineers
Engineer Topographics Laboratory
ATTN: ETL-GS-LB 1
Fort Belvoir, VA 22060

U.S. Army Topo Engineering Center ATTN: CETEC-ZC Fort Belvoir, VA 22060-5546	1
Commander USATRADOC ATTN: ATCD-FA Fort Monroe, VA 23651-5170	1
TAC/DOWP Langley AFB, VA 23665-5524	1
Commander Logistics Center ATTN: ATCL-CE Fort Lee, VA 23801-6000	1
Science and Technology 101 Research Drive Hampton, VA 23666-1340	1
Commander U.S. Army Nuclear and Chemical Agency ATTN: MONA-ZB, Bldg 2073 Springfield, VA 22150-3198	1
Record Copy	3
Total	89